Iran J Public Health, Vol. 54, No.6, Jun 2025, pp.1263-1271

Original Article

20(S)-Ginsenoside Rg3 Partially Induces Maturation of HepG2 Cells via the AMPK/HNF4A Pathway

#Li Zheng [1,2], ***#Yiheng Ding*** [3], ***Xinhao Li*** [1], ***Jingxuan Jia*** [1], ***Yanning Li*** [1,3], ****Jinsheng Qi*** [1]

1. *College of Integrated Chinese and Western Medicine, Hebei Medical University, Hebei, People's Republic of China*
2. *Department of Pharmacy, Xingtai Medical College, Hebei, People's Republic of China*
3. *Hebei Key Lab of Laboratory Animal Science, Hebei Medical University, Hebei, People's Republic of China*

***Corresponding Author:** Email: 16000636@hebmu.edu.cn
#These authors contributed equally

(Received 16 Dec 2024; accepted 21 Mar 2025)

Abstract

Background: We aimed to investigate whether 20(S)-ginsenoside Rg3 (Rg3) reduced heterogeneity by inducing the maturation of HepG2 cells via the AMP-activated protein kinase (AMPK)/hepatocyte nuclear factor 4A (HNF4A) pathway.

Methods: This in vitro cell research study was conducted under the guidance of Hebei Medical University, Hebei, China, from Sep 2022 to Dec 2023. HepG2 cells were treated with varying concentrations of Rg3 in a low glucose microenvironment. The mRNA expression of *ALBUMIN* (*ALB*, a marker for hepatocyte function) and *HNF4A* (a marker for differentiation of HCC cell), and AMPK protein levels were measured after significant changes in cell morphology were observed. Additionally, 5-Aminoimidazole-4-carboxamide1-β-D-ribofuranoside (AICAR) (an AMPK agonist) and Compound C (an AMPK inhibitor) were used to explore further the underlying mechanism.

Results: Under treatment of 5 μM, 10 μM, and 20 μM Rg3, some cells became flattened and larger, and there was an increase in the mRNA expression of *ALB* and *HNF4A* ($P<0.05$). However, there was a decreasing trend in AMPK protein content with 8 μM Rg3 ($P<0.05$). Compared to the control group, some cells exposed to 8 μM Rg3 exhibited pronounced morphological changes, along with upregulated expression of *ALB* and *HNF4A* mRNA. However, no such changes were observed when 8 μM Rg3 was combined with 1.6 mM AICAR. Compared to the control group, 10 μM Compound C or 8 μM Rg3 treatments led to similar changes in cell morphology and showed an increasing trend in *HNF4A* mRNA expression. Additionally, after treatment with Compound C, pHNF4A was mainly in the nucleus, while after Rg3 treatment, it was mostly in the cytoplasm.

Conclusion: Rg3 partially induced the maturation of HepG2 cells through the AMPK/HNF4A pathway.

Keywords: 20(S)-ginsenoside Rg3; HepG2; Maturation; Genetics

Introduction

Liver cancer poses a significant threat to human health and ranks as the third leading cause of cancer-related deaths worldwide, with hepatocellular carcinoma (HCC) accounting for over 80%

of cases (1, 2). Current treatment options primarily include immunotherapy, targeted therapies, and other approaches. However, many patients do not achieve the desired outcomes, and the mortality rate from HCC has not decreased over the past decade (3). This highlights the urgent need for novel and innovative strategies for treating HCC.

The substantial heterogeneity within HCC is a significant factor contributing to its high mortality rate, and reducing this heterogeneity could significantly benefit patients (4). Inducing HCC cells to revert to normal hepatocytes may offer a promising strategy to reduce this heterogeneity. Cytokines successfully used to stimulate the transformation of HCC cells into normal hepatocytes (5). Similarly, our previous researches demonstrated that specific stages of embryonic liver development could induce HepG2 cells to differentiate into hepatocyte-like cells (6). However, the factors that contributed to reducing heterogeneity in HCC were limited, highlighting the need to identify additional inducing factors.

As a valuable traditional Chinese medicine, *Red ginseng* is known for its ability to tonify Qi and Yang, potentially benefiting HCC patients (7). Ginsenoside Rg3 is a rare saponin derived from *Red ginseng* (8), and Rg3 has been shown to modulate the tumor microenvironment (9), enhance the effectiveness of immunotherapies (10), inhibit stemness (11, 12), and reverse epithelial-mesenchymal transition (12). Ginsenoside Rg3 may possess the potential to reduce heterogeneity in HCC cells.

Ginsenoside Rg3 exists in two isomeric forms: 20(R)- and 20(S)-ginsenoside Rg3. Additionally, 20(R)-ginsenoside Rg3 can be converted into 20(S)-ginsenoside Rg3 within the body (13). Based on this, we hypothesized that 20(S)-ginsenoside Rg3 (Rg3) was more effective for inducing HCC cell lines to mature into hepatocyte-like cells.

ALBUMIN (ALB) and HNF4A are crucial markers of mature hepatocyte-like cells. ALB, secreted by mature hepatocytes, is typically present at low levels in naive HCC cells, making it a valuable marker for identifying hepatocyte-like cells (6). Forced expression of HNF4A and other factors was shown to convert HCC cells into reprogrammed hepatocytes (14). Our research also identified HNF4A as a key molecular switch for inducing HepG2 cells to differentiate into hepatocyte-like cells (15). Therefore, we used ALB and HNF4A as markers to track the conversion of HepG2 cells into mature hepatocyte-like cells.

AMP-activated protein kinase (AMPK) is an essential upstream regulator of HNF4A (16). As a molecular switch, activation of AMPK leads to the phosphorylation of both AMPK and HNF4A. Our previous studies have also highlighted the importance of phosphorylation during this induction process (17). Consequently, we aimed to explore the inducing underlying mechanisms further from the perspective of AMPK.

To reduce the cellular heterogeneity of HCC, we induced the HepG2 cell line with Rg3, assessed cellular maturation using ALB and HNF4A markers, and evaluated AMPK protein levels. Additionally, we employed the AMPK agonist (5-Aminoimidazole-4-carboxamide-1-β-D-ribofuranoside, AICAR) and inhibitor (Compound C) to validate the proposed mechanism. This study aimed to investigate whether Rg3 could induce the maturation of HepG2 cells and the underlying molecular mechanisms. By inducing the transformation of HCC cells into normal cells, this research sought to provide a novel therapeutic option to reduce the heterogeneity of HCC cells, ultimately contributing to advancements in HCC treatment.

Materials and Methods

Study design and cell groups

In this in vitro cell research, firstly, we observed the cellular morphology of HepG2 cells treated with Rg3 (Chemfaces, Wuhan, Hubei, China) in 2022-23. Additionally, the expression of *ALB* and *HNF4A* mRNA was measured. At this stage, there were four groups: 0 μM, 5 μM, 10 μM, and 20 μM Rg3 groups.

Secondly, the AMPK protein levels in HepG2

cells treated with varying concentrations of Rg3 were investigated. The groups included six concentrations: 0 μM, 2 μM, 4 μM, 6 μM, 8 μM, 10 μM Rg3 groups.

Thirdly, the AMPK activator AICAR (Biyuntian, Shanghai, China) was added, and we observed the remodeled cellular morphology, ALB protein levels, and *HNF4A* mRNA expression. The cells were divided into the Con, (Rg3 + AICAR), and Rg3 groups at this stage.

Finally, the AMPK inhibitor Compound C (GlpBio, Montclair, CA, USA) was used, and we examined the cellular morphology, *HNF4A* mRNA expression, pHNF4A protein distribution, and cell activity in three groups: the Con group, the Rg3 group, and the Compound C group.

Drug treatment

Firstly, we reproduced the phenomenon of Rg3-induced maturation in HepG2 cells. The cells were treated with Rg3 at concentrations of 0 μM, 5 μM, 10 μM, and 20 μM for approximately 7 d. Once the changes in cell morphology were evident, the samples were collected for reverse transcription-quantitative real-time PCR (RT-qPCR) assay.

Subsequently, we investigated the underlying mechanism. The cells were co-cultured with Rg3 at concentrations of 0 μM, 2 μM, 4 μM, 6 μM, 8 μM, and 10 μM for approximately 3 d. After observing changes in cell morphology, the samples were collected for Western Blotting. Next, the cells were cultured with 0 μM Rg3, 8 μM Rg3, 8 μM Rg3 + 1.6 mM AICAR, and 10 μM Compound C for approximately 3 d. Additionally, the cells were seeded in 6-well plates with coverslips at a density of 1-5 × 10^4 HepG2 cells per well. Cell morphology was observed using an inverted microscope (Olympus, Tokyo, Japan), and the cells were fixed for immunofluorescence staining or collected for RT-qPCR and Western Blotting.

Cell culture

Cell line HepG2 was obtained from the Shanghai Cell Bank (Shanghai, China) and cultured in minimum essential medium supplemented with 20% FBS, 2 mM l-glutamine, 1 mM sodium pyruvate, 100 U/mL penicillin G sodium salt, and 0.1 mg/mL streptomycin sulfate. The cells were maintained in a conventional incubator (37 °C, 5% CO_2).

RT-qPCR

Total RNA was extracted using the RNA-Quick Purification Kit (Share-bio, Shanghai, China). Reverse transcription was performed using the All-in-One First-Strand Synthesis MasterMix (with dsDNase) kit (BestEnzymes, Lianyungang, Jiangsu, China) on a standard PCR machine (Biometra, Goettingen, Germany). Then qPCR was conducted by Taq SYBR® Green qPCR Premix (BestEnzymes, Lianyungang, Jiangsu, China) on the CFX Connect Real-Time System (BIO-RAD, CA, USA) (17). The primers used were as follows: *ALB* mRNA: sense: 5' GCTCAGTATCTTCAGCAGTGTCC 3' and anti-sense 5' GCAGTCAGCCATTTCACCATAGG 3'), *HNF4A* mRNA: sense: 5' GATGACAATGAGTATGCCTACCT 3' and anti-sense: 5' GTCGTTGATGTAGTCCTCCAA 3'), and *18S rRNA* mRNA: sense: 5' AAGTTTCAGCACATCCTGCGAGTA 3' and anti-sense 5' TTGGTGAGGTCAATGTCTGCTTTC 3'.

Western blotting

Total protein was extracted by a Seven Fast ® Column Total Protein Extraction Kit (Sevenbio, Beijing, China), quantified using a BCA kit, separated by sodium dodecyl sulfate-polyacrylamide gel electrophoresis, and transferred to a PVDF membrane via wet-transfer (300 mA, 2 h). The target proteins were detected by incubating with primary antibodies (ALB (1:300; Proteintech, Wuhan, Hubei, China), AMPK (1:300; EnoGene, Nanjing, Jiangsu, China), and Actin (1:1000; Abways, Shanghai, China)) overnight at 4 °C. Then the membranes were incubated with a secondary antibody (1:1000) 2 h at room temperature, and ECL solution for detecting. Finally, the targeted proteins were visualized and were photographed using the Licor Odyssey CLx (Licor, Lincoln, USA) for subsequent analysis (6).

Immunofluorescence

The coverslips with cells were carefully taken out. Then, the cells were fixed with 4% formaldehyde overnight, followed by permeabilization using 0.5% Triton/PBS for 15 min and blocked with 10% goat serum/PBS for 1 hour at room temperature. The cells were subsequently incubated with primary antibodies targeting pHNF4A (1:40; SAB, Greenbelt, MA, USA) overnight at 4 °C. After washing, the cells were exposed to secondary antibodies-Tetramethylrhodamine-5-(and 6)-isothiocyanate (1:20) for 2 h at room temperature. Finally, the nucleus was stained with 4', 6-Diamino-2-phenylindole dihydrochloride (DAPI). Fluorescence was detected, and images were captured using an inverted fluorescence microscope system (Nikon, Tokyo, Japan) (6).

Relative cell activities

Cell viability was assessed using the CCK-8 assay. HepG2 cells were plated at a density of 1×10^4 cells/mL in 96-well plates and treated with drugs in the medium for 48 h. Subsequently, the medium was exchanged with 10% CCK-8/media, and the cells were incubated for 30 min at 37 °C. Finally, the optical density was measured using a SuPerMax 3100 (Flash, Shanghai, China) at 450 nanometers to calculate the relative cell activities.

Statistical analysis

The data were presented as means ± standard deviation. To compare three or more groups, an analysis of variance was performed, and a two-tailed Student's t-test was used to compare the two groups. $^{*}P<0.05$ was considered to be statistically significant.

Results

Rg3-induced maturation in HepG2 cells with increased HNF4A expression

Rg3 induced maturation in HepG2 cells in a low-glucose medium (Fig. 1). When treated with 5 µM, 10 µM, and 20 µM Rg3, HepG2 cells exhibited enlarged and flattened morphology, along with other characteristics of normal hepatocyte-like cells (Fig. 1A). Compared to the control group, *ALB* mRNA expression (a hepatocyte marker) increased (Fig. 1B), and *HNF4A* mRNA expression was also elevated (Fig. 1C) with statistical difference in the 5 µM, 10 µM, and 20 µM Rg3 groups. Rg3 induced maturation of HepG2 cells within specific concentration ranges in a low-glucose environment.

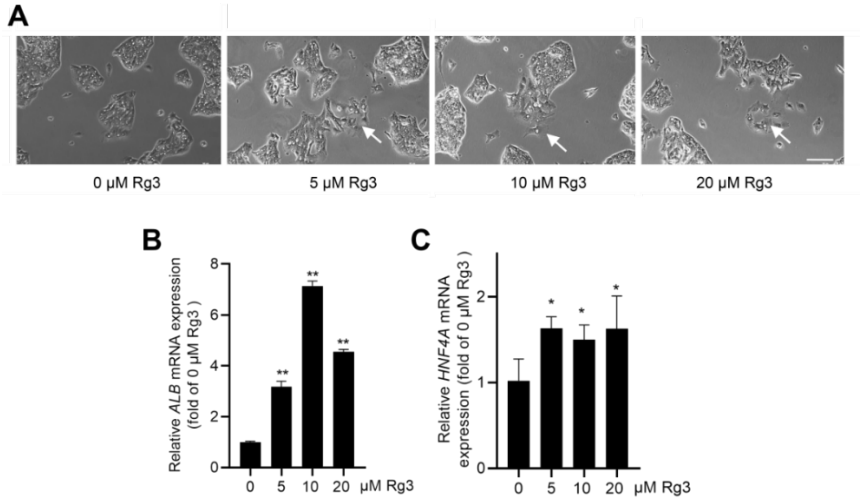

Fig. 1: Maturation of Rg3-drived HepG2 cells into hepatocyte-like cells. Rg3 induced changes in cell morphology (A). Treated with 5 µM, 10 µM, and 20 µM Rg3, the cells exhibited flattened and enlarged morphology, resembling hepatocyte-like cells (indicated by arrows). Scale bar, 50 µm. Rg3 enhanced the expression of *ALB* mRNA (B) and *HNF4A* mRNA (C), compared to the control group (0 µM Rg3). n=3, $^{*}P<0.05$, $^{**}P<0.01$

Rg3 reduced AMPK protein level in HepG2 cells

Compared with the control group, the AMPK protein level tended to decrease with 4-10 μM Rg3, with the most pronounced reduction observed at 4 and 8 μM Rg3 (Fig. 2). The AMPK protein level decreased with low concentrations of Rg3 in a low-glucose environment.

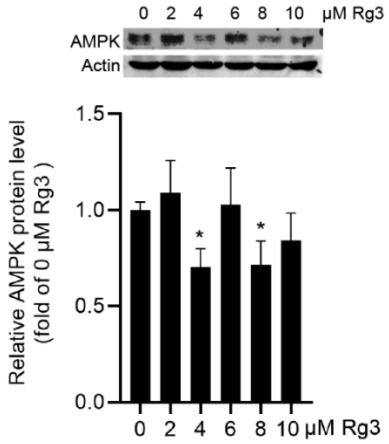

Fig. 2: Rg3 decreased AMPK protein levels, as measured under 0-10 μM Rg3 treatment, compared to the control group (0 μM Rg3), n = 3, $^{*}P<0.05$

AICAR partially blocked the Rg3-induced maturation of HepG2 cells

Compared with the control group, the cells treated with Rg3 showed altered morphology. However, the morphological changes were less pronounced in the (Rg3 + AICAR) group (Fig. 3A). Similarly, the ALB protein level and *HNF4A* mRNA expression were elevated significantly in the Rg3 group compared to the control group (Fig. 3B, C). However, compared to the Rg3 group, this increasing trend was not observed in the (Rg3 + AICAR) group (Fig. 3B, C). The maturation of HepG2 cells induced by Rg3 was partially reversed by AMPK inhibition.

Compound C played a similar role in the Rg3-induced maturation effect in HepG2 Cells

Afterward, Compound C was used to explore the underlying mechanism, and the results were as follows (Fig. 4, 5). Relating to the control group, the cell morphology changed over time in both the Rg3 and Compound C groups, with the most pronounced changes observed in the Rg3 group (Fig. 4). A similar trend was seen in the expression of *HNF4A* mRNA (Fig. 4). Treatment with Compound C resulted in the majority of pHNF4A being localized in the nucleus. In contrast, after Rg3 treatment, pHNF4A was mainly found in the cytoplasm (Fig. 5A).

Moreover, compared with the control group (Con), the relative cell viabilities in the Compound C group were decreased, whereas no such decrease was observed in the Rg3 group (Fig. 5B). This suggests that Rg3 did not function merely by inhibiting AMPK protein level, and other mechanisms may be involved in the induction process. Rg3 might act as an inhibitor of AMPK and works by increasing *HNF4A* mRNA during Rg3-induced maturation in a low-glucose environment.

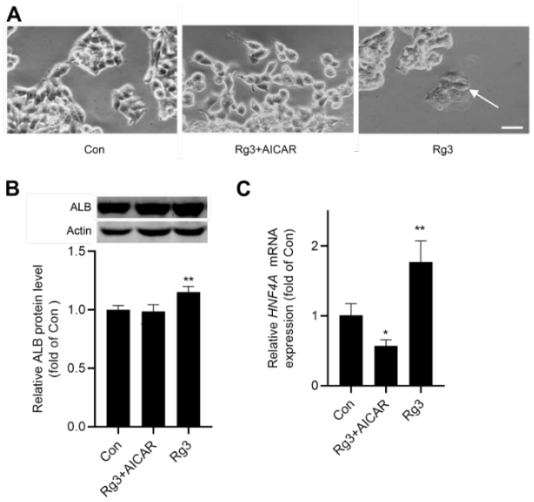

Fig. 3: AICAR partially inhibited Rg3-induced maturation of HepG2 cells. Compared to the control group, Rg3 treatment significantly altered the morphology of some HepG2 cells (A) and increased ALB protein (B) and *HNF4A* mRNA expression (C). In contrast, compared to Rg3 group, AICAR partially reversed the morphological changes (A) without increasing ALB protein (B) or *HNF4A* mRNA expression (C) in the (Rg3 + AICAR) group. Scale bar: 20 μm, n = 3; compared to the control group: $^{*}P<0.05$, $^{**}P<0.01$

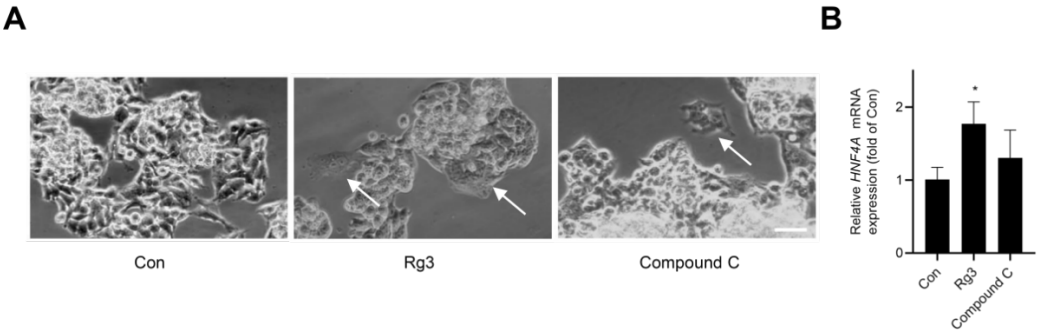

Fig. 4: Compound C produced a similar effect on inducing the maturation of HCC cells. Treatment with 10 μM Compound C or 8 μM Rg3 caused cells to become larger and more flattened (indicated by arrows) (A). Scale bar, 20 μm, compared with the control group, both Rg3 and Compound C treatments showed a trend of increased *HNF4A* mRNA expression (B). n=3, compared with the control group

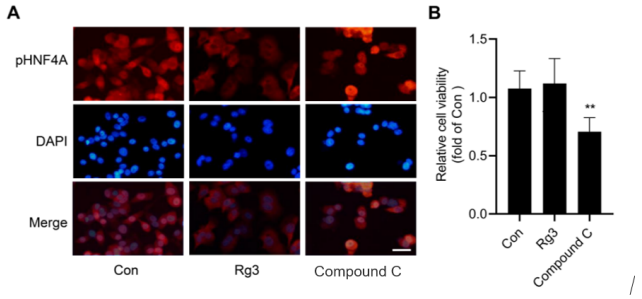

Fig. 5: Compound C and Rg3 had different effects on pHNF4A cell distribution and cell viability. Compound C (10 μM) promoted the nuclear translocation of pHNF4A, whereas Rg3 (8 μM) did not, relating to the control group (Con) (A). n=6. pHNF4A protein was shown in red, and the nucleus was stained blue with DAPI. Regarding cell activity, treatment with Compound C reduced relative cell viability, whereas Rg3 had no significant effect, compared with the control group (Con) (B), Scale bar, 50 μm, n=8, $^{**}P<0.01$

Discussion

Rg3 partially induced the maturation of HepG2 cells by upregulating HNF4A expression through the suppression of AMPK. Specifically, first, we found that 20(S)-ginsenoside Rg3 induced the maturation of HepG2 cells by upregulating HNF4A; second, the AMPK protein level decreased during this process; finally, the AMPK agonist partially reversed the maturation-inducing effect.

HCC is one of the most lethal cancers worldwide, and there is no radical treatment due to its high heterogeneity. Chinese medicine and its active ingredients are increasingly gaining attention as potential anti-tumor agents (11). In our related studies, ginsenosides exerted anti-HCC effects (18). Since Rg3 was an essential component of ginsenosides, it may induce the maturation of HepG2 cells to inhibit HCC. We therefore analyzed the effects of Rg3 on the maturation of HepG2 cells in a low-glucose medium.

First, during hepatocarcinogenesis, low-glucose environments are common due to the rapid growth of tumor cells. Increasing research suggested a close relationship between low-glucose environments and the invasion and metastasis of HCC, contributing to its high heterogeneity (19). Therefore, we cultured HepG2 cells in a low-glucose environment. In the current study, Rg3 induced a morphological transition in some HepG2 cells, increased *ALB* and *HNF4A mRNA expression,* thus driving them towards a more hepatocyte-like phenotype in a low-glucose environment (Fig. 1). Our study showed that Rg3 reduced the heterogeneity of HCC cells, which was consistent with previous research (20-22).

Second, the AMPK protein level decreased upon the treatment with Rg3 under low-glucose conditions. AMPK was activated in low-glucose environments, associated with the high heterogeneity of HCC (23). Additionally, AMPK acted as a direct inhibitor of HNF4A (24). When HepG2 cells were treated with a narrower range of Rg3 concentrations, the level of AMPK protein (a key upstream regulator of HNF4A) was decreased.

Third, AICAR partially blocked the Rg3-induced maturation of HepG2 cells, and Compound C demonstrated an induction effect similar to that of Rg3. AICAR is well known as a classic pharmacological activator of AMPK. Compared to the control group, cell morphology was significantly altered with increased ALB protein and *HNF4A* mRNA in the Rg3 group. However, no such changes were observed in the (Rg3+AICAR) group. Compound C is a recognized AMPK inhibitor. Similar morphological changes were also observed in the cells treated with Compound C and Rg3 compared with the control group. The expression of *HNF4A* mRNA exhibited an upward trend in both the Compound C and Rg3 groups. In this study, the results suggested that Rg3 induced the maturation of HepG2 cells by upregulation of HNF4A via inhibiting AMPK. This result aligned with previous studies. Huang et al. discovered that under low glucose conditions, AMPK was activated, HNF4A expression was inhibited, and the heterogeneity of HCC was enhanced (23). Our study found that Rg3 could induce the maturation of HCC cells and reduce their heterogeneity by upregulating the expression of HNF4A. In addition, other factors may also play a similar role in inducing the reduction of heterogeneity in HCC cells. For example, hepatocyte nuclear factor 1A and forkhead box protein A3 also contributed to the induction of HCC cells' transformation into normal hepatocyte-like cells (5). Our precious study also found that the specific mouse fetal liver induced the maturation of HepG2 cells by provoking the expression of HNF4A and related other transcription factors (6, 15). Moreover, the tumor supernatant from HCC cells exposed to vincristine sulfate, lnc-regulator of hepatic lineages, and tet methylcytosine dioxygenase 1 produced a comparable stimulating impact (17, 25, 26).

Finally, Rg3 partially exerted its inductive effect by upregulating HNF4A through AMPK inhibition. Although Compound C demonstrated an impact of induction similar to that of Rg3, the effects induced by Compound C and Rg3 were not identical. In the Rg3 group, pHNF4A protein

was localized in the cytoplasm, while it was detected in the nuclear in the Compound C group. Moreover, relative cell activities were reduced in the Compound C group but not in the Rg3 group. These results suggested other mechanisms might regulate HNF4A during the maturation of HepG2 cells induced by Rg3. HNF4A, a key regulator in the maturation of HCC cells, was controlled by histone demethylases (27). Additionally, phosphorylation of HNF4A was also regulated by Protein Kinase (PK)C and PKA (28), and HNF4A was subject to mRNA methylation modification and so on (29). Further investigations are needed in the later phases.

The research enhances the understanding of the processes involved in transforming HCC cells into hepatocyte-like cells, contributes to reducing the high heterogeneity of HCC, and provides further evidence for the effectiveness of Rg3 in treating HCC. At least, Rg3 may be used as an adjunct to chemoradiotherapy in patients, and a nanoscaled drug delivery system containing Rg3 could be employed to precisely deliver the drug to the liver. These approaches may lead to the best treatment outcomes for patients.

Conclusion

20(S)-ginsenoside Rg3 partially induces HepG2 cell maturation by upregulating HNF4A through AMPK inhibition.

Journalism Ethics considerations

Ethical issues (Including plagiarism, informed consent, misconduct, data fabrication and/or falsification, double publication and/or submission, redundancy, etc.) have been completely observed by the authors.

Acknowledgements

This work was supported by grants from the National Natural Science Foundation of China (82170846). It was also supported by the Natural Science Foundation of Hebei Province (H2020206328). Besides, it was also supported by the Key Research and Development Program of Hebei Province (223777133D).

Conflicts of Interest

The authors declare that there is no conflict of interest relating to this publication.

References

1. Bray F, Laversanne M, Sung H, et al (2024). Global cancer statistics 2022: GLOBOCAN estimates of incidence and mortality worldwide for 36 cancers in 185 countries. *CA Cancer J Clin,* 74(3):229-63.
2. Moradi S, Moradi G, Piroozi B et al (2021). The Burden of Cancer in a Sample of Iranian Population. *Iran J Public Health*, 50(8):1687-96.
3. Ladd AD, Duarte S, Sahin I, et al (2024). Mechanisms of drug resistance in HCC. *Hepatology*, 79(4):926-40.
4. Chan LK, Tsui YM, Ho DW, et al (2022). Cellular heterogeneity and plasticity in liver cancer. *Semin Cancer Biol*, 82:134-49.
5. Zhang X, Zhu XJ, Zhong Z, et al (2022). Small Molecule-Induced Differentiation As a Potential Therapy for Liver Cancer. *Adv Sci (Weinh)*, 9(15):e2103619.
6. Li Y, Zong Y, Xiao Z, et al (2016). Developmental Stage-Specific Embryonic Induction of HepG2 Cell Differentiation. *Dig Dis Sci*, 61(4):1098-106.
7. Zhou B, Yan Z, Liu R, et al (2016). Prospective Study of Transcatheter Arterial Chemoembolization (TACE) with Ginsenoside Rg3 versus TACE Alone for the Treatment of Patients with Advanced Hepatocellular Carcinoma. *Radiology*, 280(2):630-9.
8. Hwang SK, Jeong YJ, Cho HJ, et al (2022). Rg3-enriched red ginseng extract promotes lung cancer cell apoptosis and mitophagy by ROS production. *J Ginseng Res*, 46(1):138-46.
9. Xia J, Ma S, Zhu X, et al (2022). Versatile ginsenoside Rg3 liposomes inhibit tumor metastasis by capturing circulating tumor cells and destroying metastatic niches. *Sci Adv*, 8(6): eabj1262.
10. Sun D, Zou Y, Song L, et al (2022). A cyclodextrin-based nanoformulation achieves co-

delivery of ginsenoside Rg3 and quercetin for chemo-immunotherapy in colorectal cancer. *Acta Pharm Sin B*, 12(1):378-93.
11. Cai X, Wang Z, Lin S, et al (2024). Ginsenoside Rg3 suppresses vasculogenic mimicry by impairing DVL3-maintained stemness via PAAD cell-derived exosomal miR-204 in pancreatic adenocarcinoma. *Phytomedicine*, 126:155402.
12. Wang J, Tian L, Khan MN, et al (2018). Ginsenoside Rg3 sensitizes hypoxic lung cancer cells to cisplatin via blocking of NF-κB mediated epithelial-mesenchymal transition and stemness. *Cancer Lett*, 415:73-85.
13. Peng M, Li X, Zhang T, et al (2016). Stereoselective pharmacokinetic and metabolism studies of 20(S)- and 20(R)-ginsenoside Rg3 epimers in rat plasma by liquid chromatography-electrospray ionization mass spectrometry. *J Pharm Biomed Anal*, 121:215-24.
14. Cheng Z, He Z, Cai Y, et al (2019). Conversion of hepatoma cells to hepatocyte-like cells by defined hepatocyte nuclear factors. *Cell Res*, 29(2):124-35.
15. Li Y, Liu D, Zong Y, et al (2015). Developmental Stage-Specific Hepatocytes Induce Maturation of HepG2 Cells by Rebuilding the Regulatory Circuit. *Mol Med*, 21(1):285-95.
16. Li X, Feng L, Kuang Q, et al (2024). Microplastics cause hepatotoxicity in diabetic mice by disrupting glucolipid metabolism via PP2A/AMPK/HNF4A and promoting fibrosis via the Wnt/β-catenin pathway. *Environ Toxicol*, 39(2):1018-30.
17. Zhong Y, Qi H, Li X, et al (2020). Tumor supernatant derived from hepatocellular carcinoma cells treated with vincristine sulfate have therapeutic activity. *Eur J Pharm Sci*, 155:105557.
18. Li Y, Xiao Z, Li B, et al (2016). Ginsenoside exhibits concentration-dependent dual effects on HepG2 cell proliferation via regulation of c-Myc and HNF-4α. *Eur J Pharmacol*, 792:26-32.
19. Jo H, Lee J, Jeon J, et al (2020). The critical role of glucose deprivation in epithelial-mesenchymal transition in hepatocellular carcinoma under hypoxia. *Sci Rep*, 10(1):1538.
20. Zhao W, Ma J, Zhang Q, et al (2024). Ginsenoside Rg3 overcomes tamoxifen resistance through inhibiting glycolysis in breast cancer cells. *Cell Biol Int*, 48(4):496-509.
21. Liu H, Xie T, Liu Y (2023). Ginsenoside Rg3 inhibits the malignant progression of cervical cancer cell by regulating AKT2 expression. *Heliyon*, 9(8):e19045.
22. Li J, Yang B (2023). Ginsenoside Rg3 enhances the radiosensitivity of lung cancer A549 and H1299 cells via the PI3K/AKT signaling pathway. *In Vitro Cell Dev Biol Anim*, 59(1):19-30.
23. Huang Y, Xian L, Liu Z, et al (2022). AMPKα2/HNF4A/BORIS/GLUT4 pathway promotes hepatocellular carcinoma cell invasion and metastasis in low glucose microenviroment. *Biochem Pharmacol*, 203:115198.
24. Hong YH, Varanasi US, Yang W, et al (2003). AMP-activated protein kinase regulates HNF4alpha transcriptional activity by inhibiting dimer formation and decreasing protein stability. *J Biol Chem*, 278(30):27495-501.
25. Prabhakar B, Lee S, Bochanis A, et al (2021). lncRHL, a novel long non-coding RNA required for the differentiation of hepatocytes from human bipotent progenitor cells. *Cell Prolif*, 54(2):e12978.
26. Rodríguez-Aguilera JR, Ecsedi S, Goldsmith C, et al (2020). Genome-wide 5-hydroxymethylcytosine (5hmC) emerges at early stage of in vitro differentiation of a putative hepatocyte progenitor. *Sci Rep*, 10(1):7822.
27. Schonfeld M, Averilla J, Gunewardena S, et al (2022). Male-Specific Activation of Lysine Demethylases 5B and 5C Mediates Alcohol-Induced Liver Injury and Hepatocyte Dedifferentiation. *Hepatol Commun*, 6(6):1373-91.
28. Vető B, Bojcsuk D, Bacquet C, et al (2017). The transcriptional activity of hepatocyte nuclear factor 4 alpha is inhibited via phosphorylation by ERK1/2. *PLoS One*, 12(2):e0172020.
29. Xu Y, Zhou Z, Kang X, et al (2022). Mettl3-mediated mRNA m6A modification controls postnatal liver development by modulating the transcription factor Hnf4a. *Nat Commun*, 13(1):4555.